Left- or Right-Handed Lamellar Twists in Poly[(*R*)-3-hydroxyvalerate] Banded Spherulite: Dependence on Growth Axis

Hai-Mu Ye,[†] Jun Xu,*[,†] Bao-Hua Guo,*[,†] and Tadahisa Iwata[‡]

Institute of Polymer Science & Engineering, Department of Chemical Engineering, School of Materials Science and Technology, Tsinghua University, Beijing 100084, China, and Department of Biomaterial Sciences, Graduate School of Agricultural and Life Sciences, The University of Tokyo, Tokyo 113-8657, Japan

Received July 22, 2008; Revised Manuscript Received October 31, 2008

ABSTRACT: Novel morphology of banded spherulite was observed in poly[(*R*)-3-hydroxyvalerate) (PHV) during its isothermal crystallization at temperatures between 50 and 80 °C. A novel optical technique, Polscope was applied to obtain both the birefringence retardation and azimuth angle of the slow optical axis at each pixel in the micrograph of the polycrystalline specimen. It is revealed that two different morphological regions, normal and eye-like regions, are derived from different growth axes of the lamellae along the radial direction. In the normal region, lamellae grow and twist along *b* axis, leading to the alternative strong and weak positive birefringence. In the eye-like region, they grow and twist along *a* axis, resulting in the alternative positive and negative birefringence. It is of particular interest to note that PHV lamellae in the two regions exhibit the opposite twist senses. To the best of our knowledge, it is the first report that an optically pure chiral polymer contains two lamellar twist senses in one spherulite. We attribute the driving force of lamellar twist in PHV spherulite to the unbalanced anisotropic surface stresses. A mechanical model is proposed to interpret the opposite twisting senses along the two orthogonal growth axes. The results demonstrate that the growth axis is one of the factors determining the twist handedness of the lamellae of chiral polymers.

Introduction

Chirality is an interesting phenomenon in nature, which has been observed in the assemblies of inorganic materials,[1−3] organic materials ranging from low molecular weight compounds[4−6] to polymers,[7−9] and the more complicated biological systems.[10] Though great efforts have been devoted to the topic, it still remains a mystery as to how the chiral sense on a certain structural level is developed. Due to the definitely clear structure, the nonracemic chiral polymers provide an ideal platform to investigate the expression of chirality on the different structural levels. In this article, we will focus on the chiral sense of lamellar twist in polymer banded spherulites.

Banded spherulites consisting of cooperatively twisting lamellar crystals have been frequently observed in many polymers, both achiral and chiral. In achiral polymers, there is no preference for a certain twist handedness. Both left-handed and right-handed twists occur in each banded spherulite.[11] However, in the banded spherulites of nonracemic chiral polymer, only one twist sense has been reported, e. g., the twist sense is right-handed in the banded spherulites of poly(L-lactide) (PLLA), poly[(*R*)-3-hydroxyvalerate] (PHV), poly[(*R*)-3-hydrobutyrate-*co*-(*R*)-3-hydroxyhexanoate] (PHBHHx), poly[(*R*)-epichlorohydrin] (*R*-PECH), and poly[(*R*)-propylene oxide] (*R*-PPO), while left-handed in those of poly(D-lactide) (PDLA), poly[(*R*)-3-hydroxybutyrate] (PHB), poly[(*S*)-epichlorohydrin] (*S*-PECH), and poly[(*S*)-propylene oxide] (*S*-PPO).[9,12−16]

What determines the twist sense of the lamellar crystals of the nonracemic chiral polymers? The question has attracted a lot of researchers in the past decades and is still an open question. Singfield et al. reported that the (*R*) and (*S*) enantiomers of PECH and PPO show the opposite twist handedness,[15,16] in line with the case of synthetic silk fibroin.[17] However, there are also some exceptions that lamellar crystals with the same configurational and conformational chirality demonstrate the opposite twist handedness. For example, PHB and PHV have the same configurational chirality (with (*R*) chiral center in the main chain) and conformational chirality (both with left-handed helical chain stems in the crystalline core), but the former gives left-handed twist and the latter right-handed twist.[13] In addition, only a methylene difference in the main chain chiral liquid crystalline polyesters polymerized from (*R*)-(−)-4′-{ω-[2-(*p*-hydroxy-*o*-nitrophenyloxy)-1-propyloxy]-1-alkyloxy}-4-biphenylcarboxylic acid, PET(*R**-9) and PET(*R**-10), leads to the opposite twist handedness of the lamellar crystals though the two polymers have the same configurational chirality.[18] Keith and Padden proposed that the lamellar twist in polyethylene may result from uneven surface stresses.[19,20] Recently, on the basis of lamellar twisting and scrolling in a variety of polymers, Lotz and Cheng suggested that lamellar twist in chiral polymers is a consequence of unbalanced stresses resulting from different chain conformations on the opposite surfaces of the lamellae.[21] In the banded spherulites of PHB and PLA, the unbalanced surface stresses have been attributed to chiral (or zigzag, or staggered) folds on the lamellar surface.[9,22] Though there is no simple correlation between molecular chirality and lamellar twist sense from the previous reports, it seems that a certain chiral polymer shows a fixed handedness of lamellar twist.

In this article, we report a novel organization mechanism of polymer spherulite. PHV banded spherulite consisted of the normal region with alternative strong and weak positive birefringent bands and the eye-like region with alternative positive and negative birefringent bands. Via a recently developed polarization optical technique, PolScope,[23,24] we can quantitatively determine the birefringence retardation and the orientation of slow optical axis at each pixel in the micrograph of the polycrystalline sample, which are hard to obtain with the traditional polarized optical microscopy. PolScope reveals that in PHV spherulite the lamellae may grow with *a* or *b* axis

* To whom correspondence should be addressed. E-mail: (J.X.) jun-xu@tsinghua.edu.cn; (B.-H.G.) bhguo@tsinghua.edu.cn.
† Institute of Polymer Science & Engineering, Department of Chemical Engineering, School of Materials Science and Technology, Tsinghua University.
‡ Department of Biomaterial Sciences, Graduate School of Agricultural and Life Sciences, The University of Tokyo.

10.1021/ma801653p CCC: $40.75
Published on Web 11/18/2008

as the radial direction. It is of particular interest to note that the opposite twist senses were observed along the two orthogonal growth directions (twist axes) of the lamellar crystals in the same spherulite. To the best of our knowledge, it is the first report on both left-handed and right-handed twisting senses of the lamellae in a nonracemic chiral polymer. On the basis of the anisotropic surface stress, the mechanical model can well explain the observed phenomenon.

Experimental Section

PHV with M_w = 1 760 000 g/mol and M_w/M_n=2.8 was isolated from a recombinant *Ralstonia eutropha* harboring the PHA-biosynthesis genes of *Aeromonas caviae*.[25] The glass transition temperature and melting point were determined as T_g = −17 °C and T_m = 107 °C using a Shimadzu DSC-60 calorimeter at a heating rate of 10 °C/min.

PHV powder sandwiched between two clean glass slides was melted on a hot stage at 180 °C for 3 min, then transferred quickly to another thermal stage preset at a fixed temperature for isothermal crystallization. The digital images of the *in situ* growth process and the final morphology after complete crystallization of PHV spherulites at different temperatures were captured through a polarized optical microscope (POM) (Kerr, China) coupled with a computer controlled CCD camera (Panasonic, Japan). To obtain qualitative information of birefringence, a first order sensitive tint plate (530 nm) was inserted into the illumination path. The samples for atomic force microscopy (AFM) study were specially prepared. After complete crystallization of the PHV sample between two glass slides, the cover slide was gently removed to obtain an exposed PHV film on the bottom glass slide. Then, the specimen was mounted onto the sample stage of an SPM 9500-J3 instrument (Shimadzu, Japan). Both height and phase images were recorded simultaneously with tapping mode at room temperature. Etched silicon tips with a resonance frequency of approximately 290 KHz and a spring constant of about 18 N/m were used. Two-dimensional WAXD pattern of the sample at a selected region was obtained on a Rigaku R-Axis Spider instrument with a Mo target. The wavelength of the X-ray was 0.708 Å and the beam size was 200 μm in diameter.

The instrument design of PolScope is based on the traditional polarized optical microscope with the incident light centered at 546 nm, in which the compensator is replaced by a universal compensator made from two electro-optical liquid crystal modulators (see Figure 3 in ref 24). The modulators function as linear retarders whose retardance values are varied independently by a voltage applied to each device. The computer-controlled universal compensator, together with electronic imaging and digital image analysis, was utilized to measure the specimen birefringence in every pixel of the image. For the measurement, the birefringence of the two liquid crystal retarder plates was changed to four specific settings. For each setting, an image of the specimen was recorded. The four images were then used to compute the specimen birefringence in every pixel, based on polarimetric algorithms.[23,24,26]

Results and Discussion

Observation of Novel Banded Morphology. Melt-crystallized PHV forms banded spherulites when observed under polarized optical microscope. Crystallization temperature has a considerable effect on the spherulite morphology. When PHV was isothermally crystallized below 50 °C or above 80 °C, banded spherulites with alternative strong positive and weak positive bands were observed (Figure 1a). When crystallized at the temperatures ranging from 50 to 80 °C, PHV exhibited a novel complicated morphology, which consisted of two regions: an eye-like region (white arrow) with alternative positive and negative birefringent bands and the normal region with alternative strong positive and weak positive bands (Figure 1b). The peculiar morphology has been previously reported by Saracovan et al.;[12] however, the authors did not pay attention to the eye-like region (it was not even mentioned in the text).

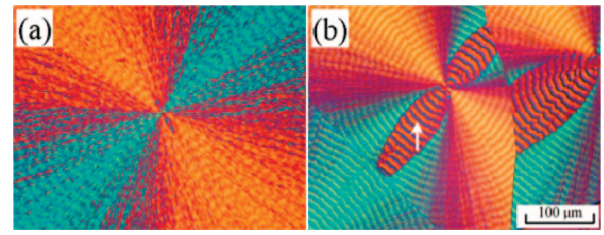

Figure 1. POM images of PHV isothermally crystallized at (a) 88 and (b) 70 °C, respectively. The white arrow indicates the eye-like region with alternative positive and negative birefringent bands.

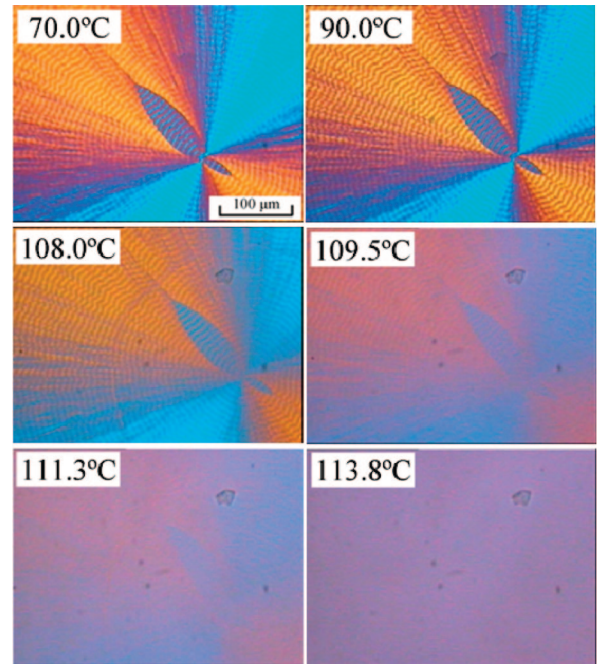

Figure 2. *In situ* melting of PHV spherulites isothermally crystallized at 65 °C. Both the eye-like region and the normal region melt simultaneously.

Banding spacing in the eye-like region is a bit larger than that in the normal region. For example, the band spacing was 8.5 μm in the eye-like region and 7.7 μm in the normal region when PHV was crystallized at 70 °C. The band spacing in the two regions increases with the crystallization temperature. As the band spacing is not the focus of this article, the data are not shown and discussed here.

To judge whether the eye-like region results from another crystal modification or the other factors, real-time melting was carried out to obtain the melting temperature range of the two regions. From Figure 2, it is clearly revealed that the eye-like region has the same melting range as the normal region, from 108 to 114 °C. Consequently, the two different regions probably have the same crystalline modification, which agrees with the fact that only one crystal modification of PHV has been reported so far in literature.[27,28]

To further investigate the crystalline structure of the eye-like and the normal region, we recorded the 2D-WAXD patterns of the two regions using an X-ray beam focused into a spot of 200 μm. The results in Figure 3 confirm that the two parts of the spherulite are of the same crystalline modification, which agrees with the reported orthogonal form with unit cell parameters: a = 0.932 nm, b = 1.002 nm and c (fiber axis) = 0.556 nm, belonging to the $P2_12_12_1$ space group.[27,28]

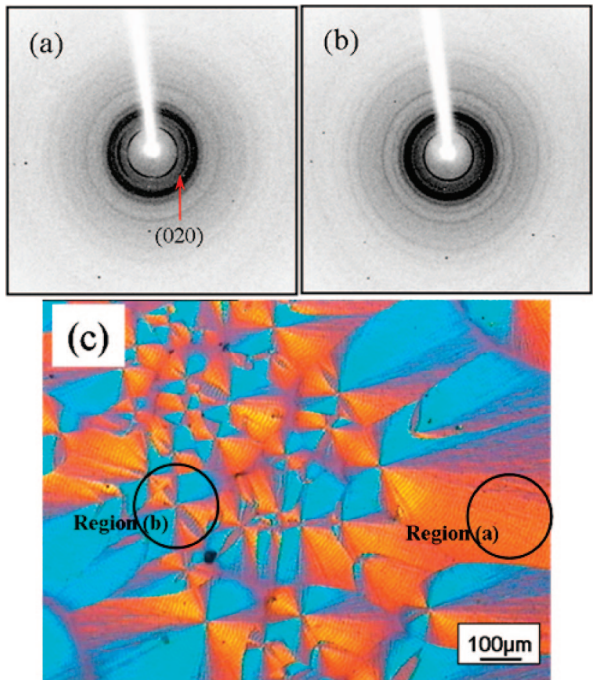

Figure 3. Selected region 2D X-ray diffraction pattern of (a) normal region of PHV spherulite, (b) center of PHV spherulite (mixture of normal and eye-like region). Only the region with a diameter of 200 μm was irradiated by the X-ray beam to obtain the diffraction pattern, and (c) the POM morphology of the sample used for selected region 2D X-ray diffraction.

Determination of Growth Axis and Twist Handedness of PHV Lamellae. To further reveal the orientation of the crystal axes in the two regions of PHV banded spherulite, we applied PolScope, a novel quantitative birefringence imaging system to characterize the PHV film. The traditional polarized optical microscope shows only the intensity of the transmitted light, which depends on both the birefringence retardation and orientation of the optical slow-axis according to the following equation:

$$I = I_0 \sin^2[2(\theta - \phi)] \sin^2(\delta/2) \quad (1)$$

where I_0 is the intensity of the linearly polarized light incident on the specimen, δ is the birefringence retardation; θ and ϕ are the azimuth of the slow optical axis of the sample and that of the polarizer, respectively. As revealed by eq 1, in the traditional POM image, δ and θ are coupled together, making it difficult to determine them separately. To solve the problem, Oldenberg and Mei developed a quantitative birefringence imaging system, which was commercialized with the trade name PolScope.[23] Via electronic controlled liquid crystal polarizer, ϕ can be varied in a fast speed so that an image can be captured in less than a few seconds. Using a set of four images collected at four sets of ϕ, we can obtain the magnitude of the birefringence retardation and the orientation of the slow-axis separately at each pixel of the PolScope image.[23,24,26]

A PHV sample crystallized at 70 °C was imaged under PolScope to reveal the two-dimensional distribution of the birefringence retardation and the azimuth angle of the slow optical axis in the specimen (Figure 4). In the normal region with all positive birefringent bands, the slow axis (with the largest refractive index) is along the radial direction; while in the eye-like region, it orients alternatively parallel and normal to the radial direction. Because the two parts are of the same crystal modification, the difference must result from the variable orientation of the lamellae. There are two possible ways of varied lamellar orientation: zigzag growth or lamellar twist.

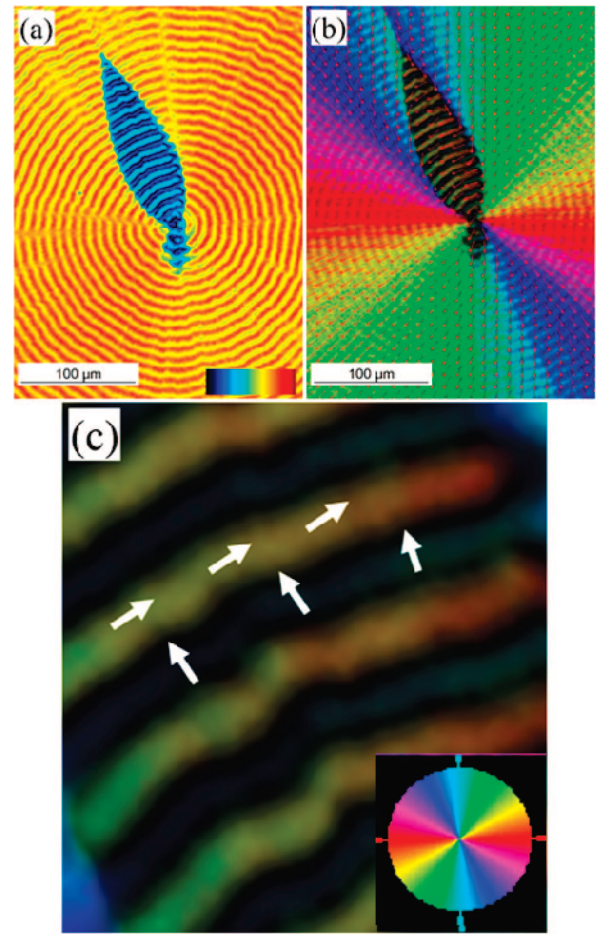

Figure 4. PolScope images of a PHV spherulite: (a) Magnitude of birefringence retardation, which is given as pseudocolor. Red corresponds to 273 nm retardance and black corresponds to zero birefringence. (b) Orientation of the slow optical axis in each location, which is typically shown by short lines for every 15 pixel in the horizontal and vertical direction of the original video frame. (c) Magnified micrograph of the eye-like region. The pseudocolor denotes the azimuth angle of the slow optical axis at each pixel. The white arrows indicate the orientation of the slow optical axis in the bands.

Zigzag growth will not lead to variance of the birefringence retardation, so lamellar twist is the most probable reason. AFM images of the normal and the eye-like region further confirm that lamellar twisting along the radial direction causes the alternative edge-on and flat-on orientation of the lamellar crystals in both the two regions (Figure 5).

The twist sense was determined by the stage tilt experiments based on the method adopted by Keith and Padden,[29] Maillard and Prud'homme.[9] A twisted lamella can be simplified as a screw. The vertical right-handed screw conducts to a visual descent of the apparent screw thread when it is rotated in right-handed direction, while inverse for a left-handed screw. For the twisted lamellae, rotation in the direction of their own twist handedness leads to a descent of the corresponding extinction bands. Namely, right-handed rotation of right-handed twisted lamellae causes a visual descent of the corresponding extinction bands and right-handed rotation of left-handed twisted lamellae results in a visual rise of the extinction bands. To achieve that, a goniometer was introduced in the microscope stage to hold the sample, and the sample was rotated around a spherulite diametric axis. By applying right-handed rotation of the PHV samples and observing the shift of the extinction bands in the two regions, it is possible to determine the twist handedness of the lamellae. To our surprise, the eye-like region shows left-handed twist while the normal region gives right-handed twist

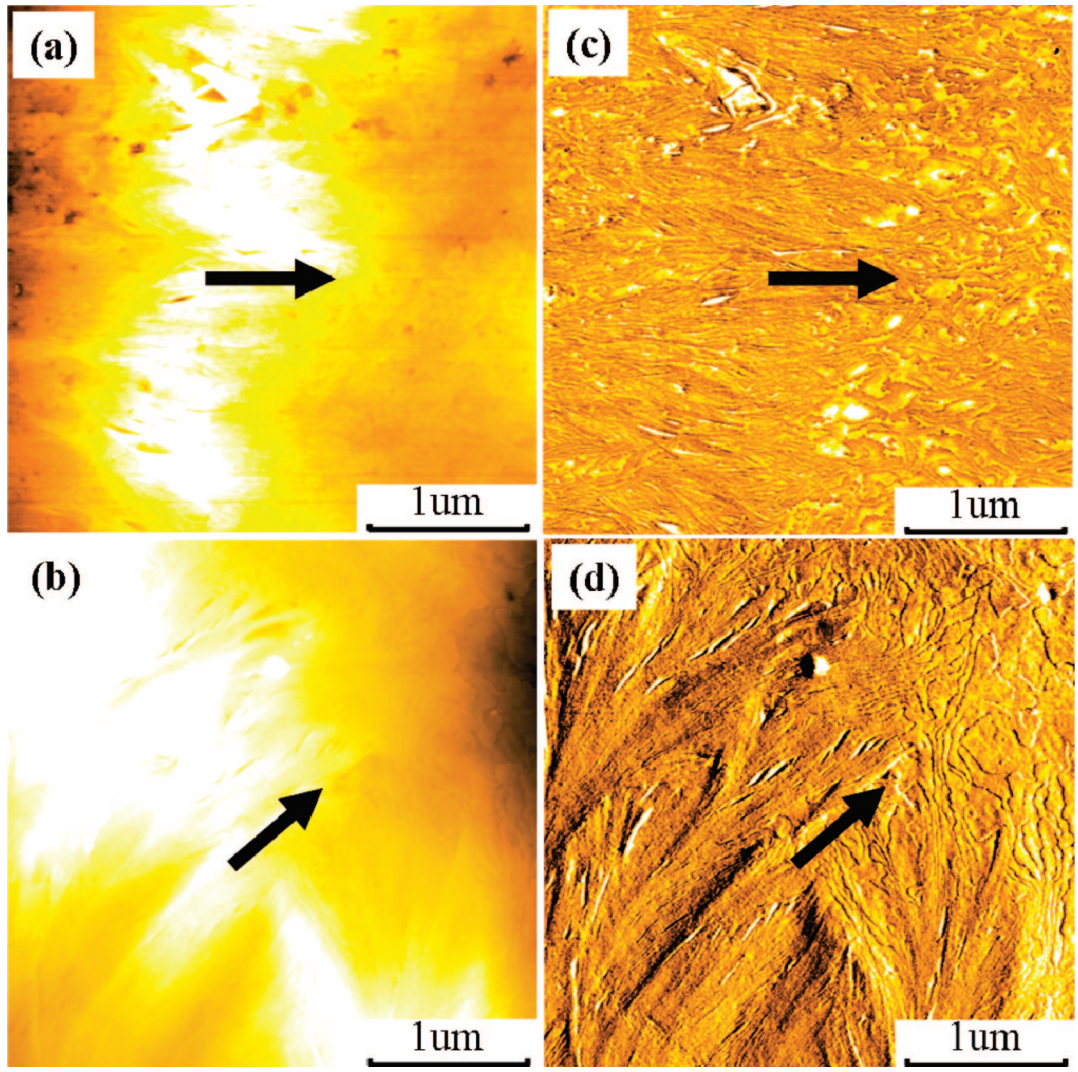

Figure 5. AFM images of the lamellae in the normal region (a and c) and in the eye-like region (b and d) of a PHV banded spherulite. The left and the right column show the height and the phase images, respectively. The arrow in each figure indicates the radial growth direction of the spherulite.

(Figure 6). The right-handed twist sense in the normal region is in accordance with the report of Saracovan et al.,[12] however, the left-handed twist sense in PHV has not been reported previously. In the nonracemic chiral polymers, existence of both twist senses of lamellae has not yet been reported, too. All the previous reports demonstrate that a certain optically pure polymer shows a certain handedness of lamellar twist, though there is no simple correlation between the configurational/conformational chirality and the lamellar twist sense. Origin of the two twist senses observed here will be interpreted in the following discussion section.

PHV is optically biaxial with three principal refractive indices n_1, n_2 and n_3. It is generally defined $n_3 > n_2 > n_1$. In the normal region of PHV spherulite, n_3 must be in the radial direction according to the PolScope result, which agrees with the positive birefringence shown in Figure 1. Saracovan et al.[12] reported that *b* axis of PHV lamellar crystals was in the radial direction, determined from the microbeam X-ray diffraction, but it was not clear whether *c* axis was associated with n_1 or n_2. Judged from the alternative positive and negative birefringent bands, n_2 is along the radial direction in the eye-like region. For the lamellar crystals forming spherulites, the *c* axis is usually in the tangential direction, so we conclude that n_1 and n_2 are associated with *c* and *a* axes, respectively (Figure 7). Microfocus X-ray diffraction study of the two regions is still in progress and expected to provide direct evidence on the orientation of the crystal axes in the two regions.

In order to understand how the eye-like region develops from the spherulite, we observed the *in situ* growth of PHV spherulite at 60, 65 and 70 °C. Since the growth process at the three crystallization temperatures is quite similar, only the growth process at 70 °C is presented here (Figure 8). The eye-like region and the normal region develop simultaneously and both originate from the spherulite center, however, the two regions show different radial growth rates. The eye-like region grows at a bit lower rate than the normal region (Figure 9). At 70 °C, the radial growth rate is 7.7 μm/s and 8.6 μm/s for the eye-like and the normal region, respectively. Relative difference is only 12%. The different growth rates make the eye-like region be surrounded by the normal region with elapsed time.

Formation Mechanism of Two Growth Axes in the Same Spherulite. Until now has usually one radial growth axis been observed in polymer banded spherulite, e. g. *b* axis in polyethylene and poly(ε-caprolactone), *a* axis in PHB, etc. Though Li et al. has reported double helical crystal with two orthogonal twisting axes in a main-chain chiral liquid crystalline polyester, PET(*R**-9),[8] the spherulites formed by the double helical crystals do not show birefringent bands. The eye-like spherulite morphology has also been observed in poly(ethylene

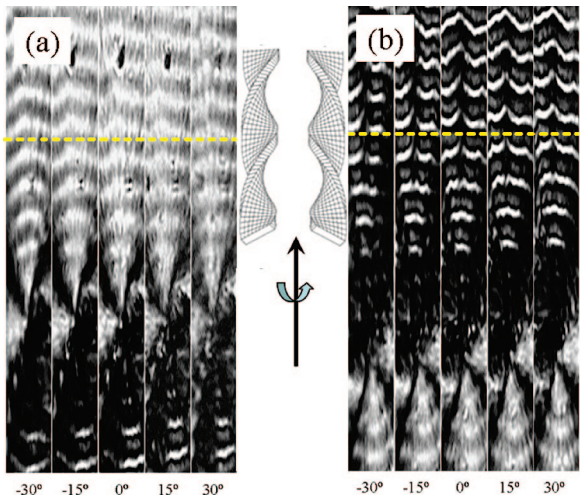

Figure 6. Sections of the banded structures observed during tilting of the sample stage in polarized optical microscope: (a) the normal region, where descent of the bands indicates right-handed twist of the lamellae; (b) the eye-like region, where rise of the bands indicates left-handed twist of the lamellae. The values at the bottom represent the angle of twist around the arrow direction in the right-handed sense. The dash line is a reference to observe the shift of the extinction band. The twisting lamellae scheme is adopted from ref 17.

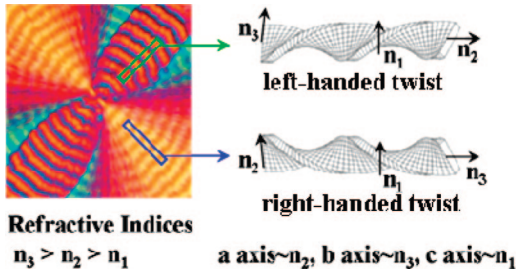

Figure 7. Scheme of the two radial growth directions and twist senses in the normal region and the eye-like region of the PHV spherulite. The twisting lamellae scheme is adopted from ref 17.

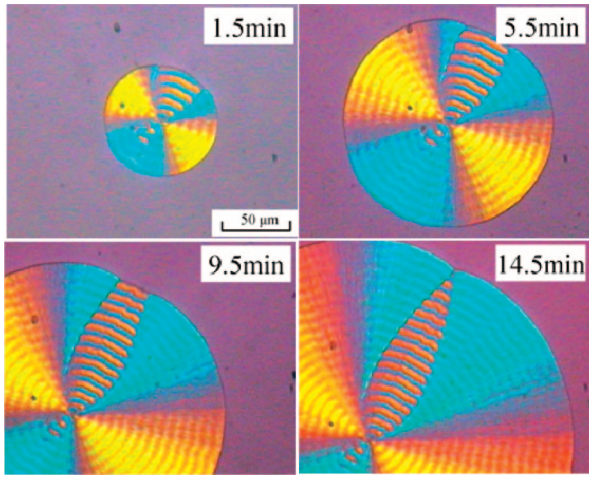

Figure 8. *In situ* growth of a PHV spherulite at 70 °C observed under POM.

succinate) (PES).[30] In contrast to PHV spherulites reported here, the eye-like regions in PES spherulites consist of flat-on lamellae surrounded by edge-on lamellae and the PES lamellae do not twist along the growth direction. In this article, via analysis of the quantitative birefringence obtained from PolScope, we find that two radial growth axes, along *a* and *b* axis of PHV lamellae can exist in the same spherulite. In the eye-like region, the

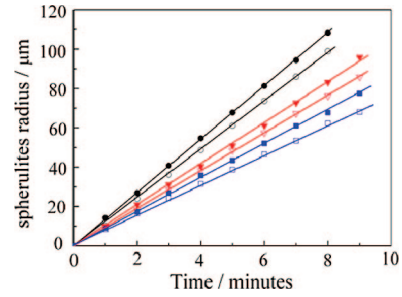

Figure 9. Growth profile of PHV spherulite crystallized at 60 °C (● normal region, ○ eye-like region), 65 °C (▼ normal region, ▽ eye-like region), and 70 °C (■ normal region, □ eye-like region).

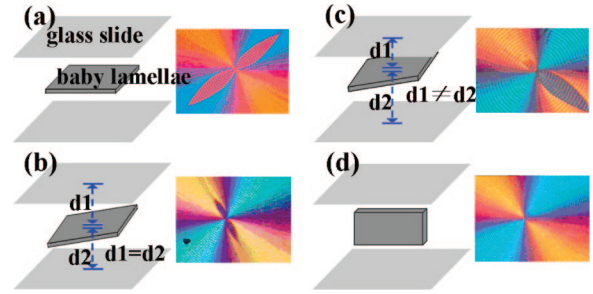

Figure 10. Formation mechanism of the eye-like morphology in PHV spherulite consisted of two radial growth axes. (a) If the baby lamellae adopt flat-on orientation, the two eye-like regions will appear symmetrically and grow to a big size, (b) if the baby lamellae are inclined to the glass slide and locate at the central plane of the film, the eye-like regions will turn smaller due to impingement with the slide but still symmetrically appear, (c) if the baby lamellae are tilted and locate nearer to the cover or bottom slide, the final spherulite will show one big and one small eye-like region, and (d) when the baby lamellae adopt edge-on orientation, the radial growth along *a* axis is constrained and the eye-like regions disappear.

lamellae twist around *a* axis; while they twist around *b* axis in the normal positive birefringent region (as Figure 7).

The formation mechanism of the peculiar morphology of PHV spherulite caused by the existence of the two radial growth axes is interpreted in Figure 10. In the early stage of the spherulite growth, the baby spherulite consists of one or several layers of single lamellar crystals. We term them as baby lamellae. If the baby lamellae are flat-on or slightly tilted against the glass slide, lamellar growth will find their way along both *a* and *b* axis. For PHV lamellae, the growth rate along *a* axis is only slightly lower than that along *b* axis. As a result, growth along *a* axis can proceed for an observable distance to form the eye-like region before engulfment by the growth along *b* axis due to growth competition. The grain boundary of the two regions is part of a logarithmic spiral, namely the ratio of the arc length to the polar radius is a constant, which equals to the ratio of the growth rate in the normal region to that in the eye-like region. The eye-like region is similar to the teardrop morphology observed in polyethylene adipate[31] and α isotactic polypropylene spherulite surrounded by the *β* spherulite due to their different growth rates.[32] Theoretical modeling of the grain boundary between the two impinging spherulites growing at different rates has been reported in literature.[31,33−35]

The radial size of the eye-like region depends on the difference in the growth rates along the two axes, the orientation and the position of the baby lamellae. The bigger difference in the growth rates along *a* and *b* axis, the smaller the eye-like region. When the lamellae in the baby spherulite adopt flat-on orientation, the two eye-like regions will appear symmetrically and grow to a big size (as Figure 10a). When the baby lamellae are inclined to the glass side, the eye-like regions turn smaller

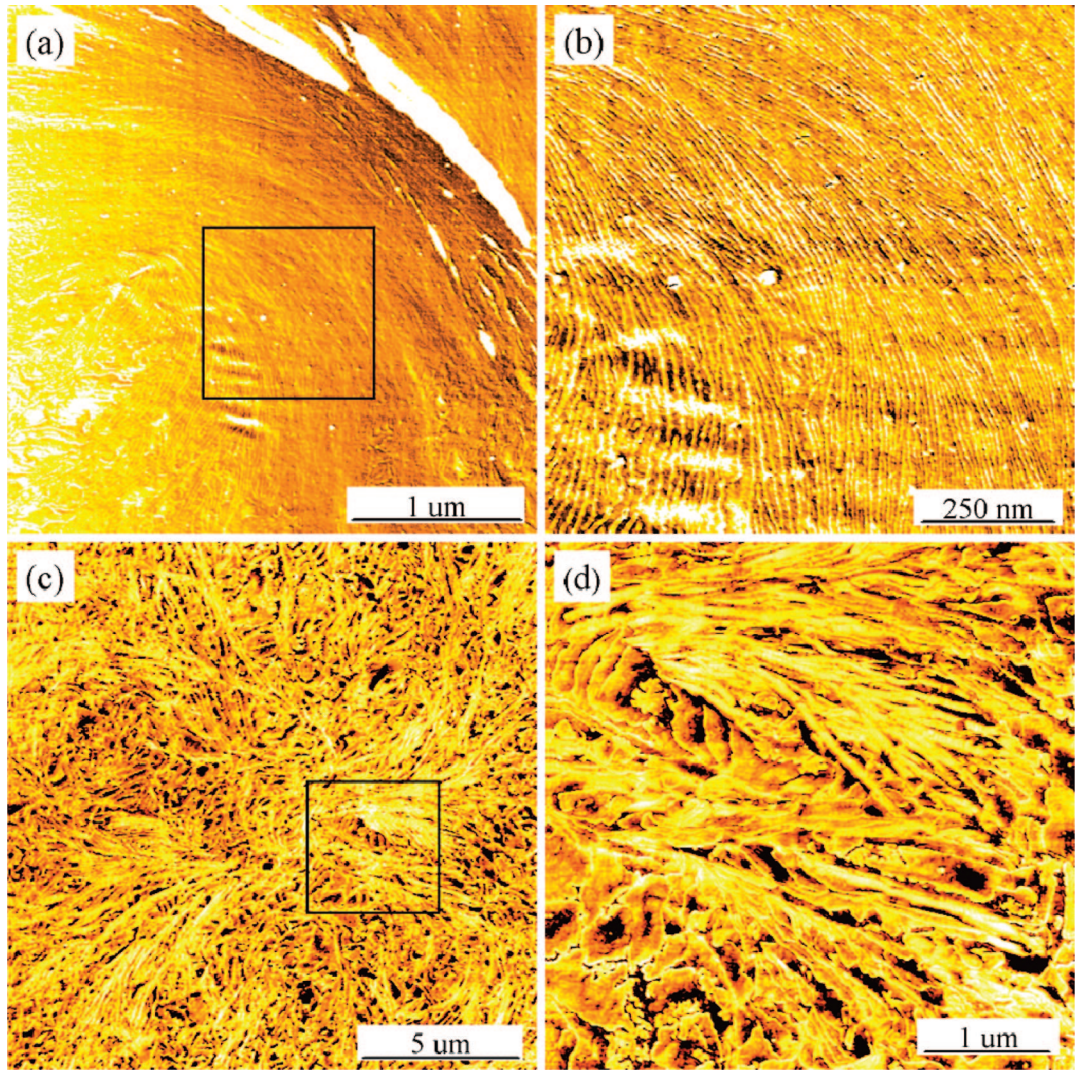

Figure 11. AFM phase images of the center of PHV spherulite (a) with only the normal morphology, and (c) with both the normal and the eye-like morphology. The two specimens were both crystallized at 70 °C. (b and d) Enlarged images of the inserted square regions in parts a and c, respectively.

due to impingement with the slide (as Figure 10b). In the case of inclined baby lamellae, if they locate nearer to the cover or bottom slide, the final spherulite will show a big and a small eye-like region (as Figure 10c). When the baby lamellae adopt edge-on orientation, lamellar growth along *a* axis is now normal to the film plane and confined by the small film thickness. The edge-on baby lamellae will branch and splay to form the skeleton of a spherulite. After they twist to flat-on orientation, the growth along *a* axis turns to the tangential direction and will soon impinge with the neighboring lamellae. As a result, the eye-like regions can not be observed (as Figure 10d). This mechanism can interpret the fact that even in the same sample, some spherulites show the eye-like regions and the others do not, as presented in Figure 3c. The proposed mechanism is confirmed by Figure 11, which shows comparison of the lamellar morphology at the center of the spherulite with and without the eye-like structure, which were crystallized at the same temperature. The center of the normal PHV banded spherulite predominantly consists of edge-on lamellae, while that of the spherulite with the eye-like structure consists mainly of flat-on or tilted lamellae. We should point out that the scheme shown in Figure 10 applies to an initial ideal single crystal nucleus. It does not include all the cases, e.g., the heterogeneous nucleation may also lead to spherulites without the eye-like regions.

Only when the growth rates along the two orthogonal axes differ a little and the lamellae adopt proper orientations, can large eye-like regions be observed. With increase of crystallization temperature, the primary nuclei are predominantly formed via heterogeneous nucleation, so the eye-like region can not be observed under POM. When PHV is crystallized at a lower temperature, the growth rate will differ more or the growing lamellae along *b* axis will splay more rapidly than those along *a* axis. As a result, the eye-like regions will not form as well. Consequently, the PHV banded spherulites with both the eye-like and normal regions could only be observed in a proper temperature range, e.g., between 50 and 80 °C.

Reason of the Opposite Twist Handedness along the Two Orthogonal Axes. Why do the lamellae twist in the opposite senses along the two orthogonal axes in PHV spherulites? We can find the answer from the origin of lamellar twist. Inspired by the suggestions proposed by Keith and Padden,[19,20] Lotz and Cheng,[21] we attribute the driving force of lamellar twist in PHV spherulite to the anisotropic surface stresses. According to the fold model proposed by Iwata and Doi,[28] the fold direction is along [1 1 0] direction at the lamellar surface. In the lamellar core, PHV chain stems adopt 2_1 helix conformation and the crystalline lattice belongs to the $P2_12_12_1$ space group. Figure 12 shows a simple model illustrating the different

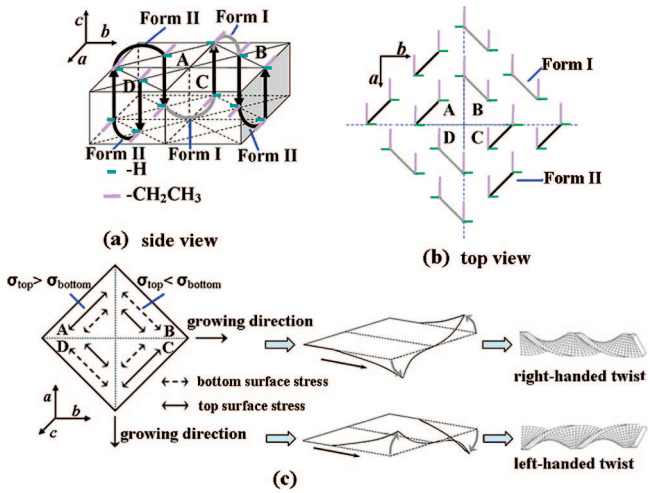

Figure 12. Mechanical model interpreting the origin of the unbalanced anisotropic surface stresses and the resultant opposite twist handedness along the two orthogonal axes of PHV lamella. (a)Side view of the configuration of the chain stems and the folds on the opposite lamellar surfaces of a single lamella, wherein the configurations are simplified according to the symmetry rule that *a*, *b* and *c* axes are the three 2_1 screw axes. A, B, C, and D indicate the four sectors of a lamella. The bold black arrows indicate the helical chain stems with up or down direction. (b) Top view of the folds on the lamellar surface. The folds of form I and those of form II are of different encumbrances. (c) Scheme of lamellar twist sense induced by the unbalanced surface stresses along the two orthogonal growth axes. The twisting lamella scheme is adapted from ref 17 and the cooperative behavior of two half-lamellae is redrawn from ref 19.

environments of the folds. The bold black arrows in Figure 12a indicate the helical chain stems, wherein the long branches and the short branches at the chiral center denote $-CH_2CH_3$ and -H groups, respectively. To be simple, we assume that the straight neighboring folds prevailed and the angle between $-CH_2CH_3$ and -H group at the chiral carbon center was 90°. The configuration schemes shown in Figure 12, parts a−c, meet the symmetry rule, namely, that the *a*, *b*, and *c* axes are the three 2_1 screw axes.

On top surface of the lamella, the folds in sector A and C are of form II and those in sector B and D are of form I. The angle between the fold of form II (abbreviated as fold II) and the two neighboring $-CH_2CH_3$ groups in the two chain stems connected by the fold is 45° and 135°. The angle between fold II and the two −H groups is 45° and 135°, too. The angle between the fold of form I (abbreviated as fold I) and the two $-CH_2CH_3$ groups is 45° and 135°. The angle between fold I and the two −H groups is 135° and 135° (Figure 12b). As a result, fold I and II encounter different encumbrances on the lamellar surfaces. Consequently, in each sector of a single lamella, the folds on the top and the bottom surface are of different encumbrances, namely, the folds on one surface are fold I and those on the opposite surface are fold II. This causes different magnitudes of the surface stresses on top and bottom lamellar surface. We define that the folds with larger angles toward the $-CH_2CH_3$ and −H groups are energetically preferred and will thus show lower surface stress. Consequently, the surface stress on top surface is larger than that on bottom surface in sector A and C, and the opposite in sector B and D. The unbalanced anisotropic surface stresses lead to bending of sector A and C with growth tip away from the observer and bending of sector B and D with growth tip toward the observer. Coupling of the curvature of the sectors leads to helicoidal twist of the lamella. When growing along *b* axis, the lamellae twist in right-handed sense; when growing along *a* axis, they twist in left-handed sense, which agree with the observed results shown in Figure 6. From the mechanical model, planar folds in the lamellar crystals of nonracemic chiral polymer will cause unbalanced surface stresses even when the chain stems are normal to the fold plane.

The two opposite twist handednesses observed in the spherulites of nonracemic PHV spherulite has pronounced effect on understanding of twisting chirality of polymer lamellae. Our report demonstrates that for the lamellar crystals of chiral polymers, the chiral sense of lamellar twist is growth axis dependent.

Conclusion

Novel spherulite morphology was observed in the melt-crystallized film of PHV. The spherulite consists of the two distinct regions: the eye-like region with positive birefringent bands and the normal region with alternative positive and negative bands. *In situ* melting and selected region wide-angle X-ray diffraction results demonstrate that the two regions have the same crystalline modification. PolScope, a quantitative birefringent imaging system was applied to determine the two-dimensional distribution of the birefringence retardation and the orientation of the slow optical axis in the spherulite. The lamellae grow and twist along *a* axis in the eye-like region, whereas they grow and twist along *b* axis in the normal region. It is of particular interest to note the opposite handedness of the lamellar twist along the two orthogonal axes. Origin of the peculiar phenomenon is successfully interpreted by a qualitative mechanical model, in which the unbalanced anisotropic surface stresses resulting from the different encumbrances of the folds on the opposite lamellar surfaces play a key role in determining the twist handedness of the lamellar crystals. Our results demonstrate that the chiral sense of the lamellar twist in chiral polymers could not be generally given, it is growth-axis dependent.

Acknowledgment. This work is supported by the National Natural Science Foundation of China (Grant Nos. 20334020, 20504019, 50673050). Dr. Jun Xu is grateful to Fisher Lu and Gina Chen from Ming-Mei Technology Co., Ltd for their help on characterization of the specimen with PolScope. The authors are grateful to Professor Bernard Lotz for his invaluable suggestions on the formation mechanism of the eye-like structure, which is adopted in the manuscript, following the review of our manuscript. We also wish to thank the anonymous reviewer for his stimulating comments on the manuscript.

References and Notes

(1) Joselewich, E. *ChemPhysChem.* **2006**, *7*, 1405–1407.
(2) Zhang, L.; Deckhardt, E.; Weber, A.; Schönenberger, C.; Grützmacher, D. *Nanotechnology* **2005**, *16*, 655–663.
(3) Zhang, L.; Ruh, E.; Grüzmacher, D.; Dong, L.; Bell, D. J.; Nelson, B. J.; Schönenberger, C. *Nano Lett.* **2006**, *6*, 1311–1317.
(4) Oda, R.; Huc, I.; Schmutz, M.; Candau, S. J.; Mackintosh, F. C. *Nature* **1999**, *399*, 566–569.
(5) Rowan, A. E.; Nolte, R. J. M. *Angew. Chem., Int. Ed.* **1998**, *37*, 63–68.
(6) Ousaka, N.; Inai, Y.; Okabe, T. *Biopolymer* **2006**, *83*, 337–351.
(7) Weng, X.; Li, C. Y.; Jin, S.; Zhang, D.; Zhang, J. Z.; Bai, F.; Harris, F. W.; Cheng, S. Z. D.; Lotz, B. *Macromolecules* **2002**, *35*, 9678–9686.
(8) Li, C. Y.; Cheng, S. Z. D.; Ge, J. J.; Bai, F.; Zhang, J. Z.; Mann, I. K.; Harris, F. W.; Chien, L.-C.; Yan, D.; He, T.; Lotz, B. *Phys. Rev. Lett.* **1999**, *83*, 4558–4561.
(9) Maillard, D.; Prud'homme, R. E. *Macromolecules* **2008**, *41*, 1705–1712.
(10) Zhou, H.; Ou-Yang, Z.-C. *Phys. Rev. E* **1998**, *58*, 4816–4819.
(11) Nozue, Y.; Hirano, S.; Kurita, R.; Kawasaki, N.; Ueno, S.; Iida, A.; Nishi, T.; Amemiya, Y. *Polymer* **2004**, *45*, 8299–8302.
(12) Saracovan, I.; Keith, H. D.; Manley, R. St. J.; Brown, G. R. *Macromolecules* **1999**, *32*, 8918–8922.
(13) Saracovan, I.; Cox, J. K.; Revol, J.-F.; Manley, R. St. J.; Brown, G. R. *Macromolecules* **1999**, *32*, 717–725.

(14) Xu, J.; Guo, B.-H.; Zhang, Z.-Z.; Zhou, J.-J.; Jiang, Y.; Yan, S.; Li, L.; Wu, Q.; Chen, G.-Q.; Schultz, J. M. *Macromolecules* **2004**, *37*, 4118–4123.
(15) Singfield, K. L.; Klass, J. M.; Brown, G. R. *Macromolecules* **1995**, *28*, 8006–8015.
(16) Singfield, K. L.; Hobbs, J. K.; Keller, A. *J. Cryst. Growth* **1998**, *183*, 683–689.
(17) Lotz, B.; Gonthier-Vassal, A.; Brack, A.; Magoshi, J. *J. Mol. Biol.* **1982**, *156*, 345–357.
(18) Li, C. Y.; Cheng, S. Z. D.; Weng, X.; Ge, J. J.; Bai, F.; Zhang, J. Z.; Calhoun, B. H.; Harris, F. W.; Chien, L.-C.; Lotz, B. *J. Am. Chem. Soc.* **2001**, *123*, 2462–2463.
(19) Keith, H. D.; Padden, F. J., Jr. *Polymer* **1984**, *25*, 28–42.
(20) Keith, H. D.; Padden, F. J., Jr. *Macromolecules* **1996**, *29*, 7776–7786.
(21) Lotz, B.; Cheng, S. Z. D. *Polymer* **2005**, *46*, 577–610.
(22) Birley, C.; Briddon, J.; Sykes, K. E.; Barker, P. A.; Organ, S. J.; Barham, P. J. *J. Mater. Sci.* **1995**, *30*, 633–638.
(23) Oldenbourg, R.; Mei, G. *J. Microsc.* **1995**, *180*, 140–147.
(24) Oldenbourg, R. *Nature* **1996**, *381*, 811–812.
(25) Fukui, T.; Kichise, T.; Yoshida, Y.; Doi, Y. *Biotechnol. Lett.* **1997**, *19*, 1093–1097.
(26) Shribak, M.; Oldenbourg, R. *Appl. Opt.* **2003**, *42*, 3009–3017.
(27) Yokouchi, M.; Chatani, Y.; Tadokoro, H.; Tani, H., Polym. J. *6* **1974**, 248–255.
(28) Iwata, T.; Doi, Y. *Macromolecules* **2000**, *33*, 5559–5565.
(29) Keith, H. D.; Padden, F. J. *J. Polym. Sci.* **1959**, *39*, 101–123.
(30) Kawashima, K.; Kawano, R.; Miyagi, T.; Umemoto, S.; Okui, N. *J. Macromol. Sci. B* **2003**, *B42*, 889–899.
(31) Point, J. J. *Bull. Acad. R. Belg.* **1955**, *41*, 974–981.
(32) Lovinger, A. J.; Chua, J. O.; Gryte, C. C. *J. Polym. Sci., Polym. Phys. Ed.* **1977**, *15*, 641–656.
(33) Lovinger, A. J.; Gryte, C. C. *J. Appl. Phys.* **1976**, *47*, 1999–2004.
(34) Schulze, G. E. W.; Wilbert, H.-P. *Colloid Polym. Sci.* **1989**, *267*, 108–115.
(35) Schulze, G. E. W.; Biremann, M. *J. Mater. Sci.* **1996**, *31*, 963–974.

MA801653P